JOURNAL OF SPACECRAFT AND ROCKETS
Vol. 42, No. 5, September–October 2005

Material Characterization of Shuttle Thermal Protection System for Impact Analyses

W.-Y. Lu,* B. R. Antoun,† J. S. Korellis,‡ and S. Scheffel§
Sandia National Laboratories, Livermore, California 94551-0969
and
M. Y. Lee,¶ R. D. Hardy,** and L. S. Costin††
Sandia National Laboratories, Albuquerque, New Mexico 87185

The purpose of this work was to obtain the mechanical behavior of the materials involved in the modeling of the foam impact scenario for the Space Shuttle *Columbia* accident investigation. The shuttle thermal protection system uses several advanced materials, including the reinforced carbon–carbon (RCC) and the high-temperature reusable surface insulation tiles (HRSI) characterized in this study. Experiments were designed to provide the modeling parameters of HRSI tiles and RCC, as well as to give insight into the failure phenomena under different loading conditions. For each material, the results are presented as a function of orientation and applied strain rate. The effect of prior flights on the RCC material properties is also discussed.

Nomenclature

A_0 = initial cross-section area, in.^{2}
D = diameter of the specimen, in.
F = magnitude of force, lb
L_0 = initial gauge length, in.
P_{Br} = peak load in "Brazilian" test, lb
T_{Br} = Brazilian tensile strength, psi
t = thickness of the specimen, in.
ΔL = change of gauge length, in.
ε_a = axial strain
ε_v = volumetric strain
σ_a = axial stress, psi
σ_f = compressive strength, psi

Introduction

THIS work represents one element of a very large effort undertaken by NASA and several supporting agencies to investigate one of the possible accident scenarios in the loss of Space Shuttle *Columbia* and its crew on 1 February 2003. In this scenario, the accident was caused by the separation of a piece of foam from the bipod ramp section of the external tank shortly after launch and its subsequent impact into the shuttle's thermal protection system.

This paper describes an experimental study that was completed to measure the mechanical material properties of the various materials that are used as an integral part of the shuttle thermal protection system. As a part of the accident investigation, NASA provided all materials to be tested. A successful numerical analysis effort of this accident scenario required experimentally determining the material properties as a function of strain rate, which had not been necessary or measured before the accident investigation. Experiments were designed to provide the modeling parameters of high-temperature reusable surface insulation (HRSI) tiles and reinforced carbon–carbon (RCC),[1] as well as to give insight into the failure phenomena under different loading conditions. Results of these experimental efforts were used to provide early preliminary analyses of foam impacting the thermal tiles and the RCC wing panels, to identify the vulnerability of the RCC panel impact, and then to perform detailed analyses to provide input for the full-scale ground testing program.[2]

Presented as Paper 2004-945 at the AIAA 42nd Aerospace Sciences Meeting, Reno, NV, 5–8 January 2004; received 15 March 2004; revision received 11 November 2004; accepted for publication 16 November 2004.

*Principal Member of Technical Staff, Mail Stop 9409, Microsystems and Materials Mechanics.
†Senior Member of Technical Staff, Mail Stop 9042, Microsystems and Materials Mechanics.
‡Member of Technical Staff, Mail Stop 9409, Microsystems and Materials Mechanics.
§Senior Technologist, Mail Stop 9721, Microsystems and Materials Mechanics.
¶Principal Member of Technical Staff, Mail Stop 0751, Geomechanics.
**Distinguished Technologist, Mail Stop 1031, Geomechanics.
††Manager, Mail Stop 0751, Geomechanics.

Thermal Tile

HRSI tiles, also known as black tiles, are made from porous silica fibers incased in reaction cured glass (RCG). They vary in thickness and densities. Two types of black tiles, LI-900 and LI-2200 (shown in Fig. 1), were used on the shuttle originally that have bulk densities of 9 and 22 lb/ft^3, respectively. LI-2200 is a higher-strength version of LI-900. Nominal dimension of the tile varies from $6 \times 6 \times 1$ to $6 \times 6 \times 4$ in. The out-of-plane (OP) direction refers to the thickness or tile depth direction, 1 or 4 in.

Three sets of experiments were conducted for porous silica material of the thermal tile: 1) uniaxial strain compression (USC) experiments to acquire data on volumetric strain response as a function of axial stress, 2) uniaxial compression (UC) experiments to identify model parameters and the rate effect of the materials, and 3) split-tension (or "Brazilian") tests to obtain the tensile strength of the material indirectly.

Porous silica tile specimens were obtained by carefully removing the RCG layer without damaging the underlying material. Because of the friable nature of the porous silica material, specimens were often sanded to the final dimension by gentle hand working.

USC

The USC test is designed to maintain zero radial strain while increasing the compressive axial load. These tests were conducted to provide volumetric-pressure relation for the HRSI tiles. The volumetric strain ε_v is measured as a function of the axial stress. Because the lateral strains are suppressed, ε_v is effectively equal to the axial strain ε_a. The USC tests were performed using a die compaction test setup as shown in Fig. 2. The test setup consists of a die, a punch, a linear variable displacement transformer (LVDT) to measure axial

Table 1 Uniaxial strain compaction experiments of HRSI tiles

Test	Density, lb/ft^3	Tile type, lb/ft^3	Sample axis orientation	Strength, psi
Tile01	9.2	9	OP	54
Tile02	9.4	9	OP	65
Tile03	9.8	9	OP	82
Tile08	7.6	9	OP	86
Tile09	9.7	9	OP	63
Tile10	9.5	9	OP	56
Tile11	10.0	9	OP	52
Tile12	8.5	9	OP	56
Tile13	8.5	9	OP	52
Tile14	20.6	22	OP	126
Tile15	20.0	22	IP	293
Tile16	20.3	22	IP	245

LI-900 tile LI-2200 tile

Fig. 1 HRSI tiles, which protect the shuttle against temperatures between 1200 and 2500°F.

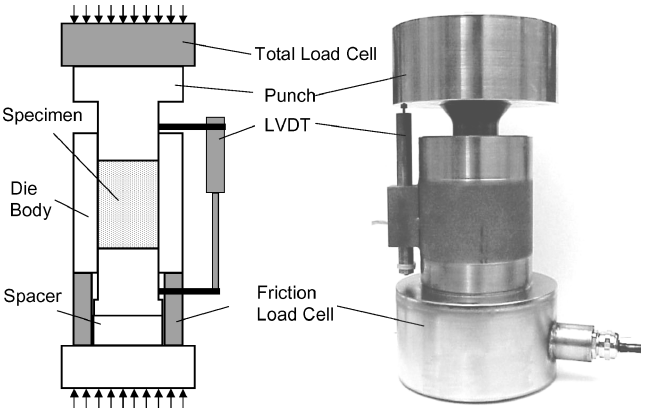

Fig. 2 Uniaxial strain test setup consisting of die, piston, and load cells.

deformation of the specimen, a total-load load cell to measure the axial load applied to the specimen and the die setup, and a frictional load cell to measure the frictional force between the specimen, the punch, and the die body. The load applied to the specimen is calculated from the total load minus the frictional load.

Right cylinder specimens were used for USC tests. The diameter of the specimen was 1.125 in. to fit the bore of the compaction die, and the length of the specimens varied from 0.625 to 1.135 in.

There were 12 USC tests (9 LI-900 specimens and 3 LI-2200 specimens) conducted. The axial stress vs volumetric strain (σ_a–ε_v) curves are shown in Figs. 3 and 4 for LI-900 and LI-2200, respectively. The test configurations are summarized in Table 1.

The σ_a–ε_v plot consists of three segments. The first segment is the elastic response of the material with a steep increase of σ_a until the specimen fails at the compressive strength σ_f. The peak stress is usually accompanied by a small amount of stress drop that may indicate a formation of compaction bands, a common phenomenon in porous materials.[3] The next segment is crush, where the localized failure propagates throughout the specimen, converting the intact material into fine powder. This segment is characterized by an increase of ε_v up to about 0.5 without increasing the applied stress significantly. The last segment is the compaction of powdered material characterized by a rapid increase in the applied stress without significantly increasing ε_v.

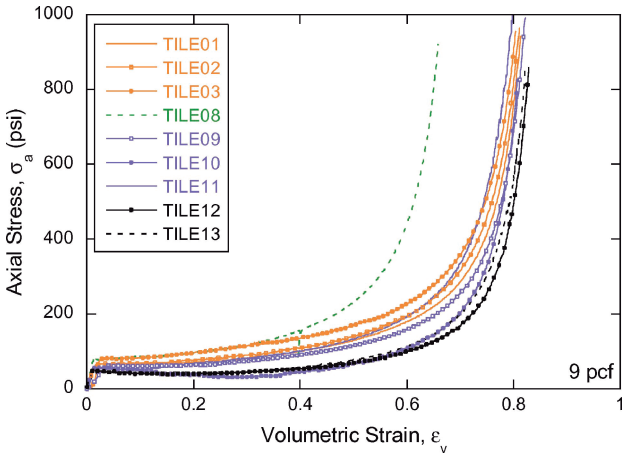

Fig. 3 Axial stress vs volumetric strain curves obtained in USC testing of LI-900.

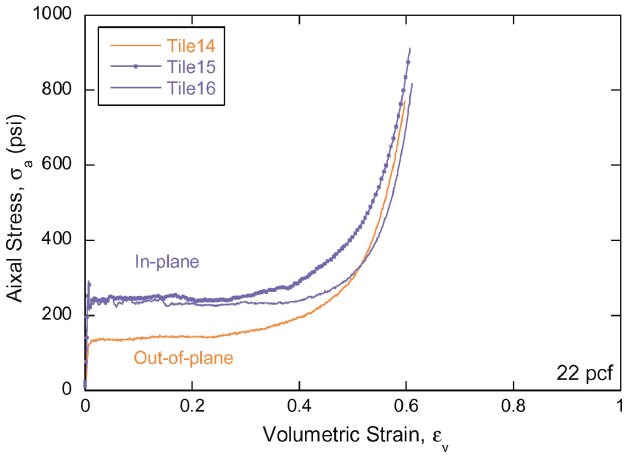

Fig. 4 Axial stress vs volumetric strain curves obtained in USC testing of LI-2200, including IP and OP loading directions.

Under USC test conditions, the value of σ_f varies from 52 to 86 psi for LI-900 in the OP loading. The strength of LI-2200 ranges from 126 to 293 psi depending on the orientation. Specimens aligned with in-plane (IP) orientation are approximately twice as strong (σ_f) compared to the OP specimen (Tile14).

UC and Strain Rate Effect

Compression specimens with a nominal size of 0.6 × 0.6 × 1.0 in. were used to study the rate effect of porous silica tile material. This set of experiments included three strain rates, 0.01, 1.0, and 200/s, and two loading directions, IP and OP. The strain rate 0.01 and 1.0/s tests were conducted on a MTS 858 frame with a TestStar IIm control system. During an experiment, the unconfined specimen was compressed to more than 40% under a constant strain rate and then unloaded. The 200/s tests were conducted on a high-rate MTS system with a shear pin breakoff fixture, the specimen was attached to the top platen, and a pretest separation of 1 in. between the bottom specimen surface and bottom platen allowed full acceleration before contact. At least three specimens were tested for each loading condition.

Experimental results of LI-900 are shown in Fig. 5. Figure 5 includes three parts, and each one displays three IP and three OP compression tests of a constant strain rate. Notice that the elastic modulus and compressive strength in the OP direction are always less than those of the IP direction. In the crush region, the OP direction shows increasing crush strength, that is, hardening, whereas the IP direction

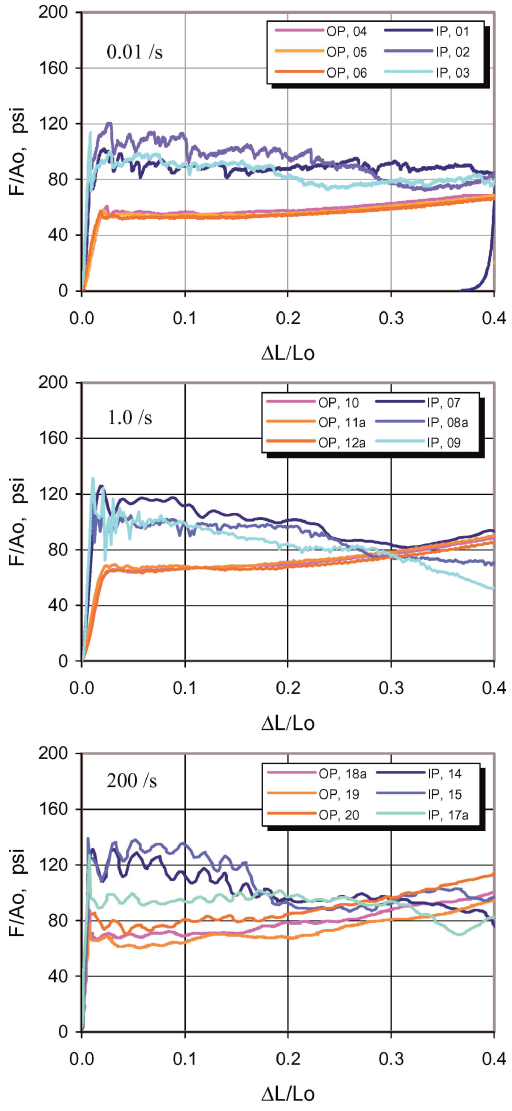

Fig. 5 Compression engineering stress-strain curves of LI-900 at strain rates 0.01, 1.0, and 200/s.

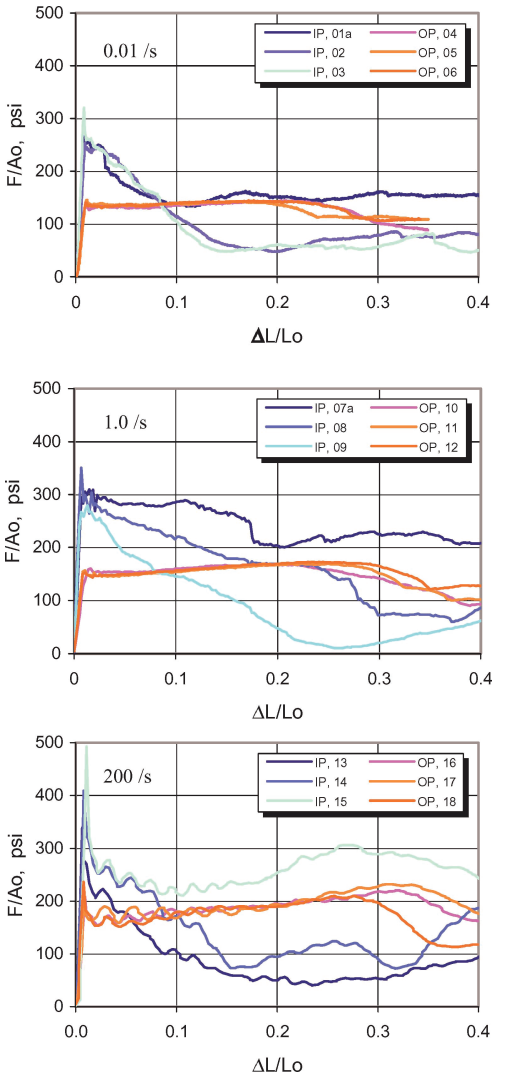

Fig. 7 Compression engineering stress-strain curves of LI-2200 at strain rates 0.01, 1.0, and 200/s.

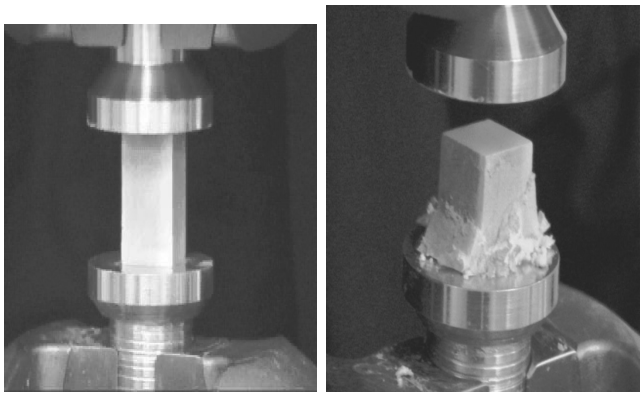

a) Undeformed specimen **b) Crushed specimen**

Fig. 6 Pre- and postexperiment of specimen 9212_01 (LI-900, IP, 0.01/s).

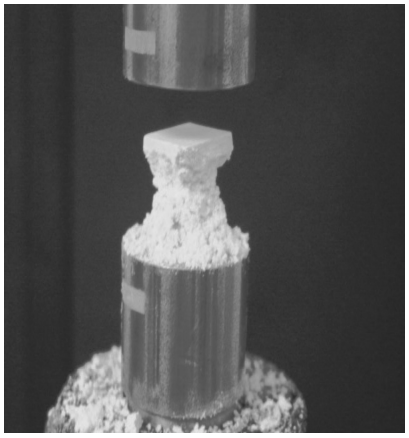

Fig. 8 Postexperiment photograph of specimen 8009_12 (LI-2200, OP, 1.0/s).

exhibits softening. An OP specimen usually retained its rectangular shape after the compression and unloading cycle; however, it would crumble when removed from the platen. During crush, IP specimens typically crumbled and cracked in shear as shown in Fig. 6.

The results of LI-2200, shown in Fig. 7, have similar trends, except that OP specimens do not show continuous hardening. The crush strength of OP specimens first increases with the compressive strain and then falls off when spalling occurs. Figure 8 shows OP specimen 8009_12 immediately following completion of the test at a strain rate of 1.0/s. Significant spalling of various size fragments occurred during the experiment, evidenced by high-speed photography.

The IP and OP elastic moduli for LI-900 are about 4.0 and 16 ksi, respectively, and they were 160 and 330 ksi for LI-2200.

The effect of strain rate can be observed in both Figs. 5 and 7. Note that the compressive strength increases with strain rate. The strength

vs strain rate of thermal tiles is shown in Fig. 9. Experimental data are more scattered when the strain rate is higher and also when loading is in the IP direction.

Split Tension (or Brazilian) Test

Split tension tests were conducted to estimate the tensile strength of the HRSI tile. This test was chosen to measure approximate properties in a very quick manner that was sufficient for the planned modeling. Three disk-shaped specimens were prepared from the 3-in.-thick LI-900 tile; the dimensions of the specimens were 1.5 in. in diameter and 0.9 in. thick, nominally. A diametrical line indicating the loading axis was marked on the specimen to align the specimen in the loading machine. The compressive line load was applied to the specimen at a constant diametrical strain rate of 10^{-3}/s.

The indirect tensile strength of the material was calculated from the following equation:

$$T_{\mathrm{Br}} = 2P_{\mathrm{Br}}/\pi t D \tag{1}$$

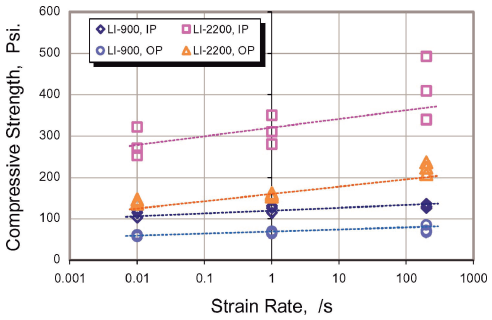

Fig. 9 Relation of compression strength and strain rate of thermal tiles.

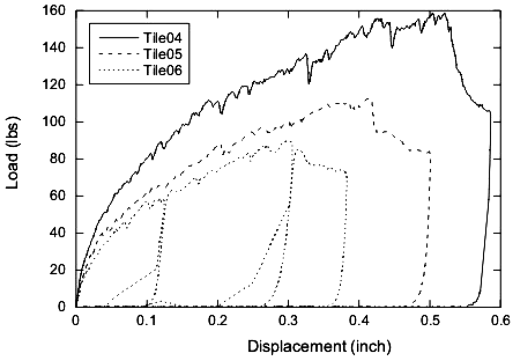

Fig. 10 Diametrical displacement vs load plots obtained from the Brazilian indirect split-tension test of LI-900 specimens.

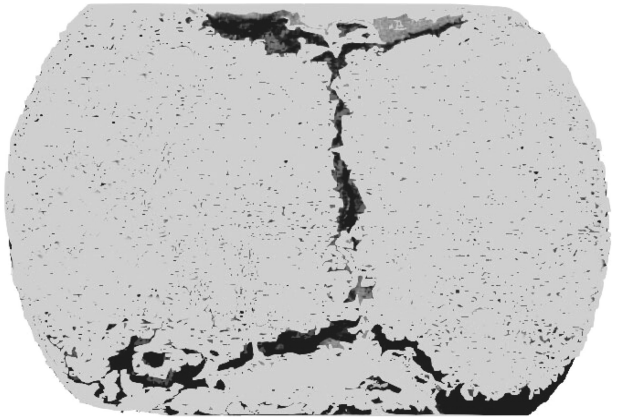

Fig. 11 Typical fracture pattern induced in HRSI tile specimen under diametrical loading.

where T_{Br} is the indirect Brazilian tensile strength in pounds per square inch, P_{Br} is the peak load in pounds, t is the thickness of the specimen in inches, and D is the diameter of the specimen in inches.

Figure 10 shows the Brazilian test records for three specimens; the diametrical load-displacement curves are displayed. The calculated values of T_{Br} are 78, 64, and 42 psi for Tile04, 05, and 06, respectively. The tensile failure of the HRSI tile material was initiated after the large deformation of the specimen (from 0.3 to 0.5 in.). Figure 11 shows a deformed specimen with typical extension fractures formed along the loading axis. Because of the large diametrical deformation of the specimen, the shear fractures were formed near the contact surfaces of the specimen with the loading pistons. These subsidiary shear fractures[4] and large deformation of the specimen may only allow us to use the value of T_{Br} as the rough estimate of tensile strength of the HRSI tile material.

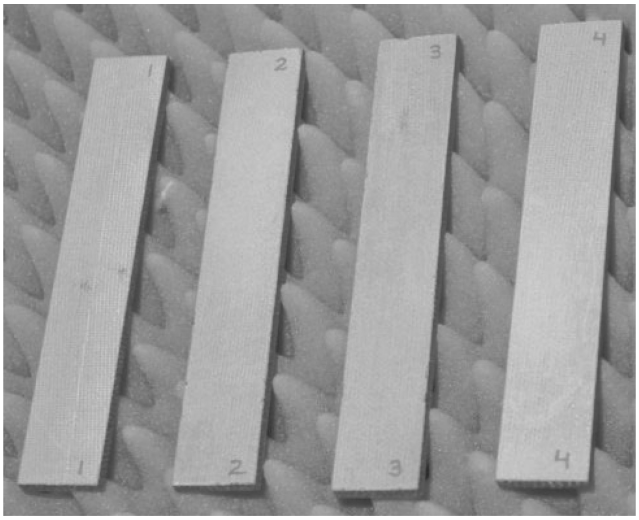

a)

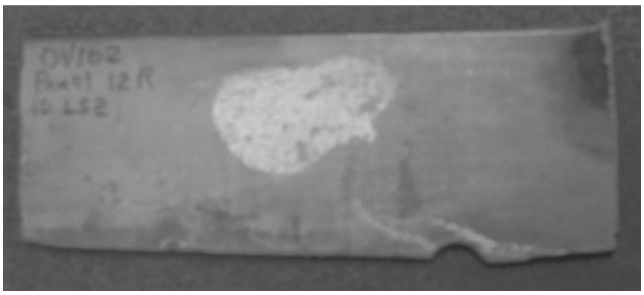

b)

Fig. 12 Examples of a) pristine (0-flight) and b) 19-flight RCC material provided by NASA for characterization.

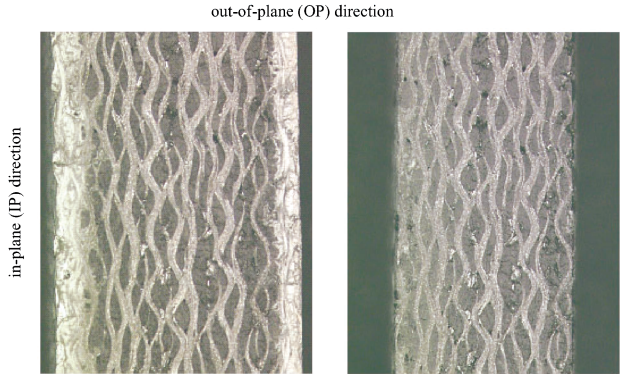

Fig. 13 RCC composite cross section as received and after removal of SiC coating.

RCC

The RCC composite material used on Space Shuttle *Columbia* is manufactured into large panels in the shape of the leading edge of the wings. There are 22 RCC panels of varying size and shape that make up the leading edge of each wing, providing structural strength over the extreme range of temperatures encountered during flight missions.[5] During reentry into Earth's atmosphere, the leading edge is exposed to temperatures up to 3000°F. Oxidation of RCC material varies with temperature, pressure, and environment, and, therefore, oxidation effects vary with wing location as well as within individual panels. The outer surfaces of the RCC panels are converted into SiC during the manufacturing process to provide oxidation resistance to minimize substrate mass loss and associated strength loss during reentry.[5]

RCC material was provided in small sections of various sizes for the material characterization experiments. RCC material was provided in pristine condition (RCC1, RCC2, RCC3, and RCC5) and from leading-edge wing panels 10 left, 12 right, and 15 right (RCC10L, RCC12R, and RCC15R). Additionally, materials 1S and LS1 (RCC1S and RCCLS1) were from wing panel 10 left and

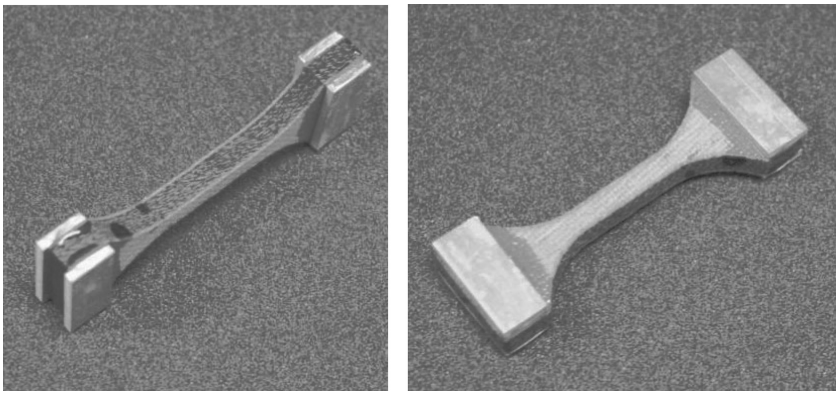

Fig. 14 RCC tensile specimen with aluminum tabs bonded on grip section.

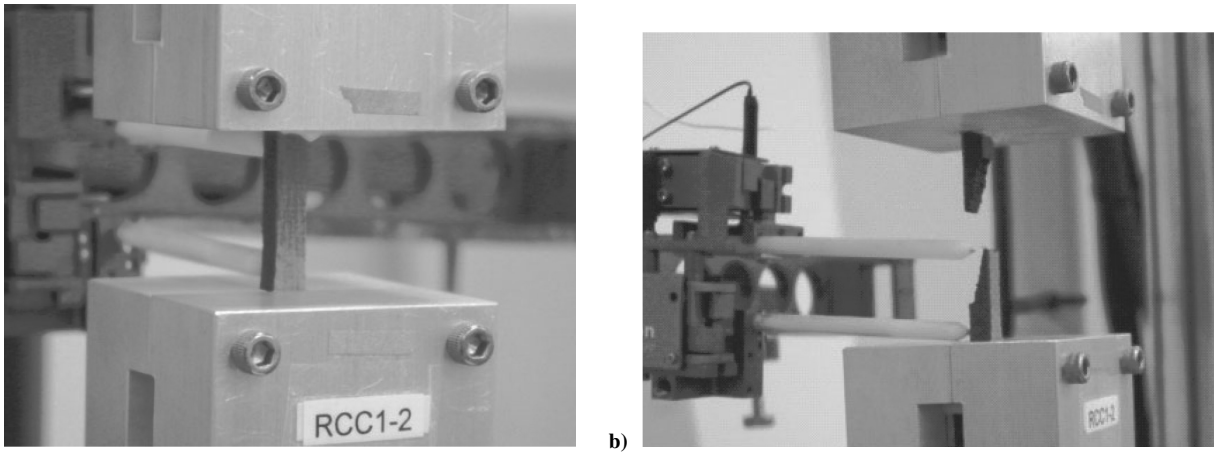

Fig. 15 Tensile specimen RCC1-2 a) before and b) after tensile experiment.

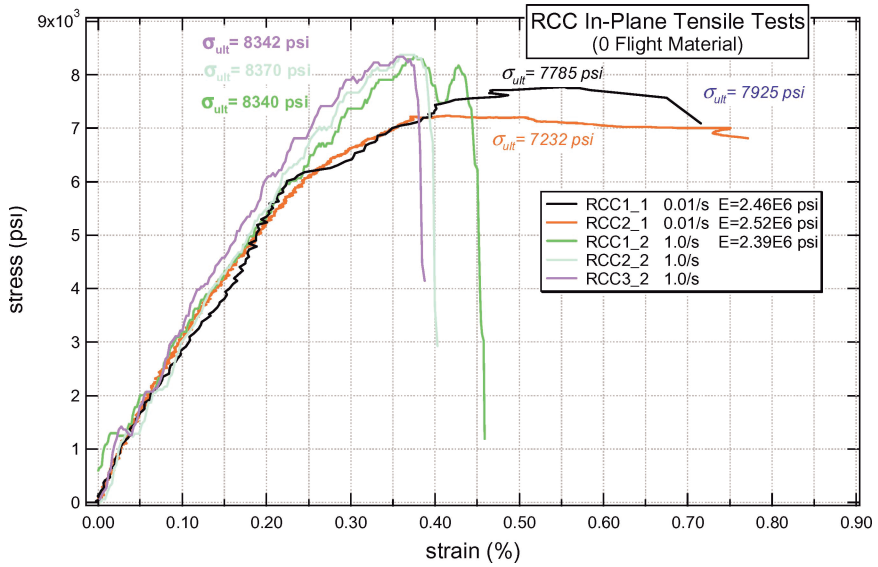

Fig. 16 IP tensile results for pristine (zero-flight) RCC.

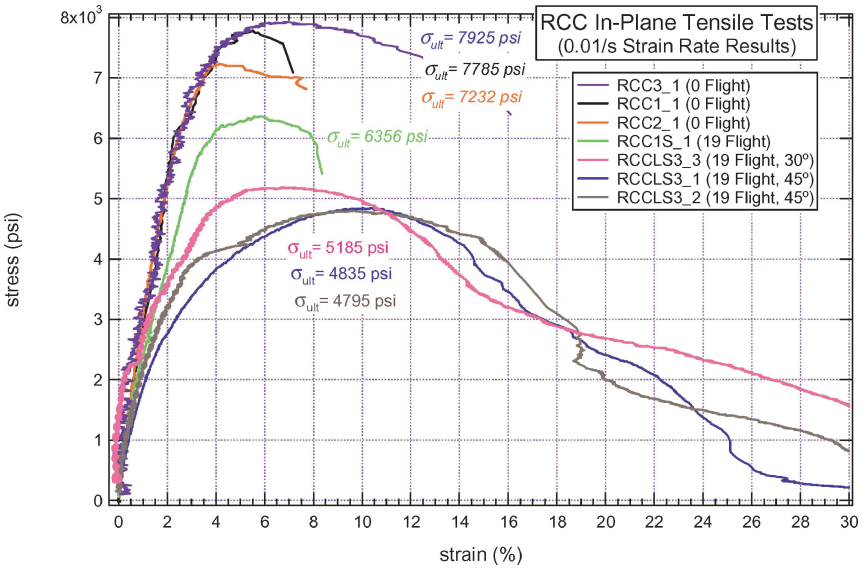

Fig. 17 IP tensile results for pristine (0-flight) and 19-flight RCC at 0.01/s strain rate and various orientations.

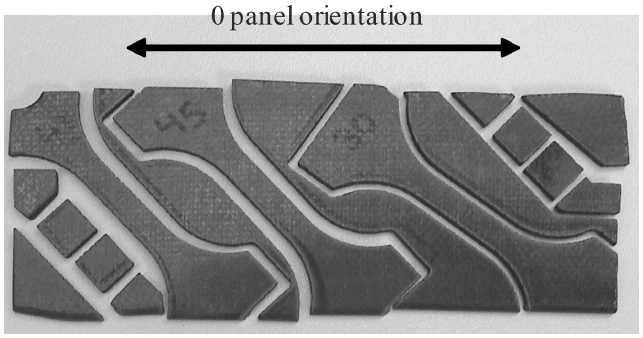

Fig. 18 RCC panel LS3 tensile and compression specimen removal layout.

material LS2 (RCCLS2) was from wing panel 12 right. All of the leading-edge wing panel material was removed from Space Shuttle *Columbia* after 19 flights of service, as part of the panel refurbishment schedule.[5] Examples of typical RCC samples received in both pristine (0-flight) and 19-prior-flight conditions are shown in Fig. 12. All RCC material was 19-ply with a nominal thickness of 0.25 in. and an average density of 92 lb/ft^3. The SiC layers on the composite surface comprised approximately 25% of the total thickness, as can be seen in Fig. 13.

Three types of experiments were conducted on RCC: 1) tension experiments to determine tensile strength as a function of strain rate and orientation, 2) compression experiments to determine IP and OP properties as a function of strain rate, and 3) IP bending experiments to determine rate effects. The effect of prior flights on material properties was also evaluated for each of the three experiment types, an important effect because *Columbia* was on its 28th mission and possessed RCC panels with varying mission histories.[5]

Specimens were abrasive water-jet machined from the RCC panel samples with an effort to maximize specimens from the very limited available material. Orientation of each material section was typically marked and was verified by surface and edge evaluation under an optical microscope.

RCC Tension Experiments

Tensile specimens had an overall length of 2.9 in. with an 0.8-in. gauge length and a 0.25-in. gauge width, shown in Fig. 14. IP 0-deg orientation experiments were conducted at three strain rates, 0.01, 1.0, and 200/s. Additionally, off-axis (30- and 45-deg) experiments were conducted at 0.01/s to determine orientation effects. The 0.01 and 1.0/s strain rate experiments were conducted on an MTS 858

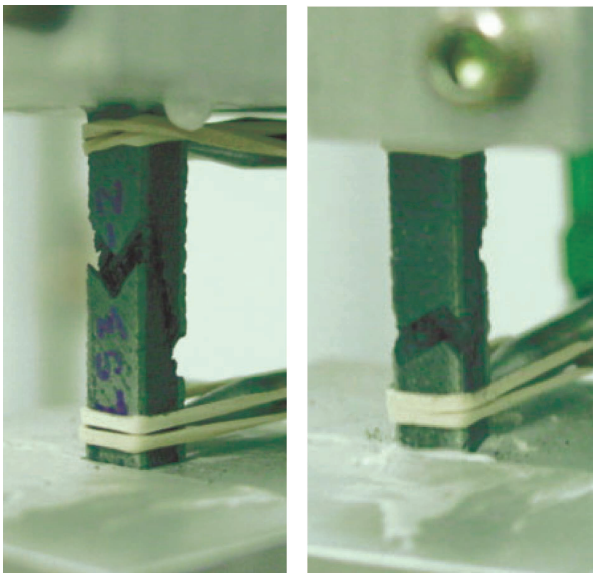

a) b)

Fig. 19 Failure of a) 45-deg specimen RCC LS3-2 and b) 30-deg specimen RCC LS3-3.

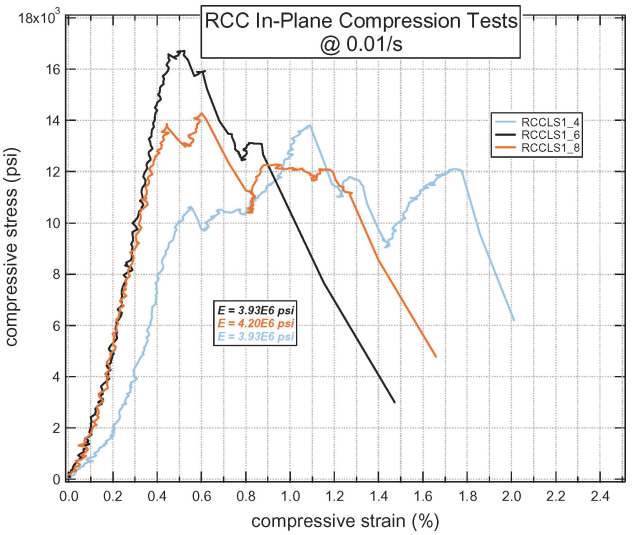

Fig. 20 IP compression results for 19-flight RCC material panel LS1.

test frame with a TestStar IIm control system, and the 200/s experiments were conducted on an MTS high rate test frame in open-loop control. Custom grips were designed that allowed each specimen to be aligned and epoxy cured in place in either test system to ensure successful tests. All specimens failed within the gauge section. Specimen RCC1-2 is shown in Fig. 15 before and after testing.

The tensile results for the pristine (zero-flight) RCC are shown in Fig. 16. The measured IP elastic modulus was 2.4E6 psi on average, and the ultimate tensile strength varied from about 7.2 to 7.9 ksi.

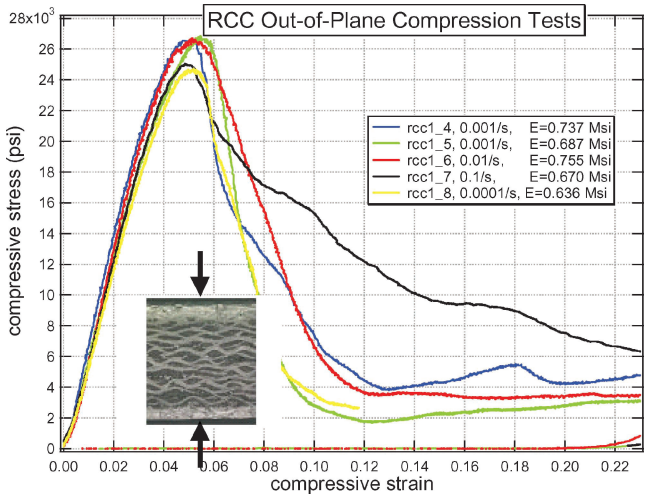

Fig. 21 OP compression results for 19-flight RCC material panel LS1.

Specimens taken from the same sample panel were tested at two rates. The tests conducted at higher strain rates, 1.0/s, had higher ultimate tensile strengths, about 5% higher than 0.01/s, and also failed at about one-half the failure strain of the 0.01/s strain rate. A comparison of tensile properties at 0.01/s strain rate is shown in Fig. 17. Specimens removed from panel material that had been exposed to 19 flights exhibited about 15% lower ultimate tensile strength values than specimens from pristine material. Also shown

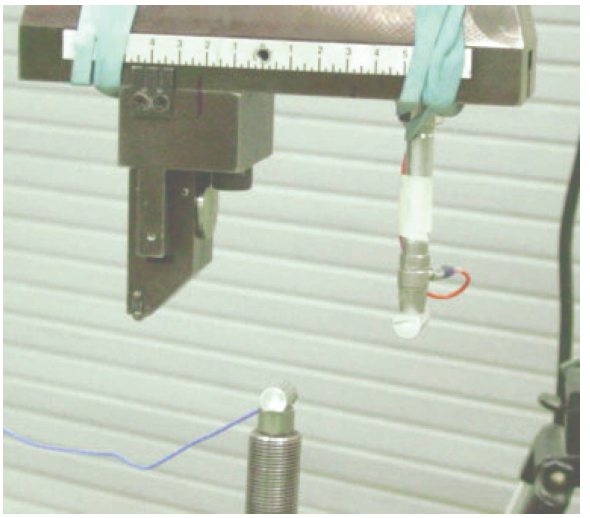

Fig. 24 High rate three-point bend setup with load cells on two loading points.

a) **b)**

Fig. 22 Three-point bend RCC specimen a) before and b) after failure.

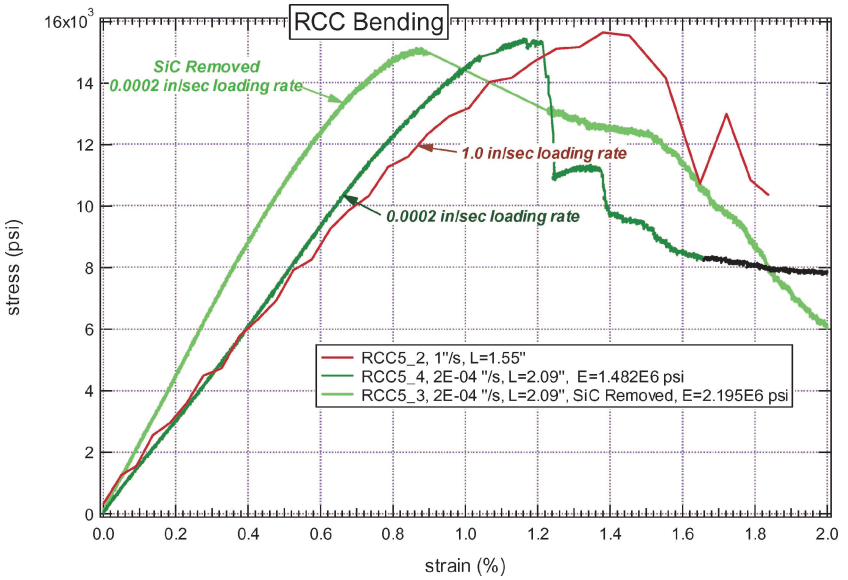

Fig. 23 RCC slow rate three-point bend results.

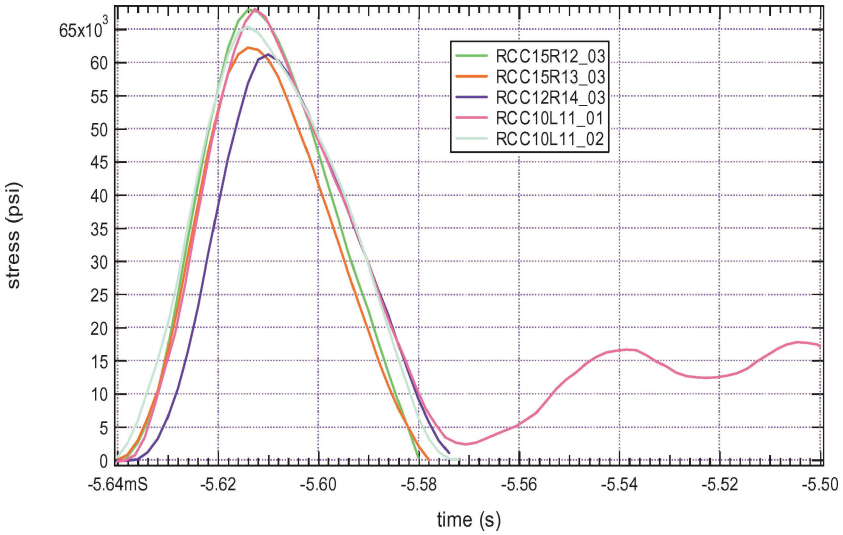

Fig. 25 High rate three-point bend results for 19-flight RCC material.

in Fig. 17 is a comparison of orientation on tensile behavior for 19-flight RCC material. An 18 and 24% lower ultimate tensile strength than the 0-deg orientation specimen was measured in the 30- and 45-deg orientation specimens, respectively. A photograph of the specimens removed at 30- and 45-deg orientations from RCC panel LS3 is shown in Fig. 18, and Fig. 19 shows the dependence of fracture angle on tensile orientation.

RCC Compression Experiments

Compression specimens were sized and located to optimize material use in each RCC sample panel and measured approximately 0.4-in.^{2} by 0.25-in. nominal thickness; variations in dimensions did not affect the measured properties. Experiments were conducted in two orientations, IP and OP, which is in the thickness direction. Early experiments showed no rate dependence in IP compression between the strain rates of 0.001/s and 0.1/s. IP and OP compression tests were all conducted on an MTS 880 test frame with a TestStar II control system. IP specimens required careful hand sanding following the water-jet machining procedure to produce good results.

Results from three IP compression experiments from RCC sample panel LS1 (19 flights, wing location unknown) are shown in Fig. 20. The elastic modulus in IP compression was about $4E6$ psi, compared to $2.4E6$ psi in the same orientation in tension. There was considerable scatter in compressive strength due to the brittle nature of the material and possibly the flight oxidation effects. The highest IP compressive strength measured on this 19-flight RCC material was about 16 ksi, compared to 7.6–8.6 ksi measured on the same panel in tension. Additional experiments were conducted on specimens after removing the SiC layers (Fig. 13). No significant effect on either elastic modulus or compressive strength was measured after accounting for dimension reduction.

Figure 21 shows results from several OP compression tests with specimens from RCC sample panel 1 (pristine, 0 flights). No strain rate dependence was noted over the range of tests, from 0.0001/s to 0.1/s. The elastic modulus in OP compression was about 0.64–$0.75E6$ psi, or less than 10% of the IP compression modulus. The OP compressive strength measured between 24 and 27 ksi. Experiments to examine the effect of loss of the SiC layer showed a possible increase in modulus and slight decrease in compressive strength, but more testing is needed due to scatter in the results.

RCC Three-Point Bend Experiments

Three-point bend specimens were initially sized for a minimum 2-in. span length with a 0.3-in. beam width, to conserve limited material. This specimen size was used for the slower rate bend experiments, up to 1.0 in./s loading rate. Tests up to this loading rate were conducted on an MTS 858 load frame with a TestStar IIm control system. A bend specimen before and after failure is shown in Fig. 22. High rate bend experiments were conducted on an MTS high rate test frame in open-loop control at 200 in./s. Specimen dimensions for the high rate tests were a span length of 5 in. and beam width of 0.5 in.

Figure 23 shows results from the lower loading rate bend experiments for panel RCC5, pristine material. Comparing specimen RCC5_4 at 0.0002 in./s with specimen RCC5_2 at 1.0 in./s, there is no load rate effect in the material. Specimens RCC5_4 and RCC5_3 are conducted at the same loading rate, but before testing the latter specimen the SiC coating was removed from both surfaces. The measured elastic modulus increased about 50% with removal of the SiC, but no change in strength was measured (failure load scaled with dimension changes); bending failure strength over this range of loading rates was about 15 ksi.

Several high rate three-point bend experiments were performed at 200 in./s on specimens from 19-flight RCC material from panels RCC15R (panel 15 right), RCC10L (panel 10 left), and RCC12R (panel 12 right). These experiments served to validate the RCC material model and selected parameters,[2] not as material characterization experiments. The large specimen size precludes obtaining several samples from the same panel. The bend setup was changed slightly from the low rate experiments, shown in Fig. 24. Two load cells were used to measure load at two loading points, and this allowed monitoring of inertial loading that occurs at this high rate. Results from several experiments are shown in Fig. 25. At the high rate, the failure stress increased to 60–65 ksi, compared to 15 ksi in the slower tests. However, these values include high-rate inertial loading, which at 200 in./s was measured as close to one-half of the measured load.

Summary

Experiments were conducted to characterize the mechanical behavior of RCC and HRSI tiles under various loading conditions. Material orientation and rate effects were considered for all materials. Under USC test conditions, the compressive strength of LI-900 varies from 52 to 86 psi in the OP loading. LI-2200 is much stronger than LI-900. Specimens aligned with IP orientation are approximately twice as strong compared to the OP specimen. The results of UC show similar trends. The compression strength of the thermal tiles is affected by the strain rate, an approximately 10% increase from 0.01/s to 1.0/s and from 1.0/s to 200/s. The tensile strength of LI-900 obtained from a Brazilian test ranges from 42 to 78 psi.

Pristine, or zero-flight, RCC material was determined to have an ultimate tensile strength of 7.2–7.9 ksi at a strain rate of 0.01/s and exhibited some strain rate dependence. Results from 19 mission flights of oxidation-induced degradation showed about 15%

lower ultimate tensile strength values than pristine RCC material. The measured modulus in IP compression was higher than that measured in tension ($4E6$ vs $2.4E6$ psi), probably due to the crazed SiC surface[5] that can carry load better in compression than in tension. IP compressive strength was measured in the 14–16 ksi range, or about double the tensile strength. OP compressive strength measured 24–27 ksi. No notable strain rate effect was measured in IP or OP compression between the 0.0001/s and 0.1/s range. Similarly, no rate effect was measured in the bending experiments until very high loading rates, where inertial loading must be considered.

The results of this study were used in modeling the foam impact scenario for the Space Shuttle *Columbia* accident investigation.

Acknowledgments

Sandia National Laboratories is a multiprogram laboratory operated by Sandia Corporation, a Lockheed Martin Company, for the U.S. Department of Energy under Contract DE-AC04-94AL85000. We thank Glenn Miller of NASA Johnson Space Center for supplying all of the shuttle materials for testing. We also thank Kenneth Gwinn, Rodney May, Arthur Ratzel, and Kenneth Wilson for technical discussions and valuable input and Sam McFadden and Y. R. Kan for reviewing the manuscript.

References

[1]NASA Facts, Obiter Thermal Protection System, FS-2000-06-29-KSC, March 1997.

[2]Gwinn, K. W., and Metzinger, K. E., "Analyses of Foam Impact onto the Columbia Shuttle Wing Leading Edge Panels Using Pronto3D/SPH," AIAA Paper 2004-942, Jan. 2004.

[3]Olsson, W. A., "Theoretical and Experimental Investigation of Compaction Bands in Porous Rock," *Journal of Geophysical Research*, Vol. 104, No. B4, 1999, pp. 7219–7228.

[4]Jaeger, J. C., and Cook, N. G. W., "Fundamentals of Rock Mechanics," Methuen, London, 1969, pp. 169–173.

[5]Columbia Accident Investigation Board, NASA Rept. Vol. 1, Aug. 2003.

S. Bouslog
Associate Editor

Color reproductions courtesy of Sandia National Laboratories.